

TCF7L2 (Transcription Factor 7-Like 2) Regulation of GATA6 (GATA-Binding Protein 6)-Dependent and -Independent Vascular Smooth Muscle Cell Plasticity and Intimal Hyperplasia

Roshni Srivastava,* Harshvardhan Rolyan,* Yi Xie, Na Li, Neha Bhat, Lingjuan Hong, Fatemehsadat Esteghamat, Adebowale Adeniran, Arnar Geirsson, Jiasheng Zhang, Guanghao Ge, Marcelo Nobrega, Kathleen A. Martin, Arya Mani

Objective—TCF7L2 (transcription factor 7-like 2) is a Wnt-regulated transcription factor that maintains stemness and promotes proliferation in embryonic tissues and adult stem cells. Mice with a coronary artery disease–linked mutation in Wnt-coreceptor LRP6 (LDL receptor-related protein 6) exhibit vascular smooth muscle cell dedifferentiation and obstructive coronary artery disease, which are paradoxically associated with reduced TCF7L2 expression. We conducted a comprehensive study to explore the role of TCF7L2 in vascular smooth muscle cell differentiation and protection against intimal hyperplasia.

Approach and Results—Using multiple mouse models, we demonstrate here that TCF7L2 promotes differentiation and inhibits proliferation of vascular smooth muscle cells. TCF7L2 accomplishes these effects by stabilization of GATA6 (GATA-binding protein 6) and upregulation of SM-MHC (smooth muscle cell myosin heavy chain) and cell cycle inhibitors. Accordingly, TCF7L2 haploinsufficient mice exhibited increased susceptibility to injury-induced hyperplasia, while mice overexpressing TCF7L2 were protected against injury-induced intimal hyperplasia compared with wild-type littermates. Consequently, the overexpression of TCF7L2 in LRP6 mutant mice rescued the injury-induced intimal hyperplasia.

Conclusions—Our novel findings imply cell type-specific functional role of TCF7L2 and provide critical insight into mechanisms underlying the pathogenesis of intimal hyperplasia.

Visual Overview—An online [visual overview](#) is available for this article. (*Arterioscler Thromb Vasc Biol.* 2019;39:250-262. DOI: 10.1161/ATVBAHA.118.311830.)

Key Words: cell cycle ■ cell differentiation ■ hyperplasia ■ mice, laboratory ■ mutation

Advances in medical therapy, such as widespread use of lipid-lowering agents led to a significant decline in prevalence of coronary artery disease (CAD) mortality over previous 4 decades. The recent rise in cardiovascular death has generated renewed interest in identifying novel disease risk factors.¹ A parallel rise is observed in prevalence of type 2 diabetes mellitus (T2DM) and obesity, which markedly increases the risk of myocardial infarction and restenosis. The pathogenesis of T2DM-linked CAD is most likely distinct from those extensively studied in animal models of severe hyperlipidemia and inflammation, necessitating new disease models. Recent studies, including genome-wide association study (GWAS) of CAD and myocardial infarction, have implicated altered differentiation of vascular smooth muscle cells (VSMC) in pathogenesis

of CAD.^{2,3} VSMC are the most abundant cell type and have the highest degree of plasticity among all vascular cells.⁴⁻⁶ The phenotypic switching of VSMC allows their migration into the intima where they continue proliferating and depositing extracellular matrix⁷ or transdifferentiate into other cell types, such as CD68 positive and foam cells.⁸ Whether VSMC proliferation has a beneficial or detrimental role in atherosclerosis process is controversial. VSMCs may have a protective role against plaque rupture by stabilizing the fibrous cap. In a unique form of CAD, known as plaque erosion, VSMCs play a greater role than inflammatory cells in plaque formation.⁹ VSMC dedifferentiation and proliferation contribute not only to atherosclerosis but also complicate revascularization procedures, promoting restenosis postangioplasty and intimal hyperplasia at anastomoses in

Received on: August 28, 2018; final version accepted on: December 5, 2018.

From the Yale Cardiovascular Research Center (R.S., H.R., Y.X., N.L., N.B., L.H., F.E., J.Z., G.G., K.A.M., A.M.), Department of Pathology (A.A.), Department of Surgery (A.G.), Department of Genetics (A.M.), Yale School of Medicine, New Haven, CT; and Department of Human Genetics, University of Chicago, IL (M.N.).

*These authors contributed equally to this article.

The online-only Data Supplement is available with this article at <https://www.ahajournals.org/doi/suppl/10.1161/ATVBAHA.118.311830>.

Correspondence to Arya Mani, MD, Yale Cardiovascular Research Center, Yale School of Medicine, 300 George St, New Haven, CT. Email arya.mani@yale.edu

© 2018 The Authors. *Arteriosclerosis, Thrombosis, and Vascular Biology* is published on behalf of the American Heart Association, Inc., by Wolters Kluwer Health, Inc. This is an open access article under the terms of the Creative Commons Attribution Non-Commercial-NoDerivs License, which permits use, distribution, and reproduction in any medium, provided that the original work is properly cited, the use is noncommercial, and no modifications or adaptations are made.

Arterioscler Thromb Vasc Biol is available at <https://www.ahajournals.org/journal/atvb>

DOI: 10.1161/ATVBAHA.118.311830

Nonstandard Abbreviations and Acronyms

CAD	coronary artery disease
ChIP	chromatin immunoprecipitation
GATA6	GATA-binding protein 6
GWAS	genome-wide association study
LDLR	low-density lipoprotein receptor
PDGF-BB	platelet-derived growth factor-BB
SM-MHC	smooth muscle cell myosin heavy chain
T2DM	type 2 diabetes mellitus
TCF7L2	transcription factor 7-like 2
VSMC	vascular smooth muscle cells
WT	wild type

bypass grafts. The molecular mechanisms maintaining or perturbing VSMC differentiation are poorly understood.

The highly conserved Wnt signaling pathway regulates fundamental processes in embryonic development including cell fate and has been implicated in carcinogenesis.¹⁰ Recently, Wnt signaling has been implicated in regulation of VSMC differentiation.¹¹ We have previously shown that mutations in the gene encoding, Wnt-coreceptor LRP6 (LDL receptor-related protein 6) underlie autosomal dominant CAD and T2DM in humans (OMIM: ADCADII). Mice with the CAD-linked *LRP6* mutation (*LRP6^{R611C}*) exhibit coronary and aortic intimal hyperplasia, even in the absence of mechanical vascular injury, largely accounted for by excess VSMC proliferation in the absence of excess inflammation.¹¹ Disease pathway analysis in *LRP6^{R611C}* mice revealed that enhanced noncanonical Wnt signaling enhances PDGF signaling and promotes VSMC dedifferentiation and proliferation and is associated with reduced expression of the Wnt-regulated transcription factor TCF7L2 (transcription factor 7-like 2). Wnt3a administration to the *LRP6^{R611C}* mice reduced PDGF signaling activities, normalized TCF7L2 expression, and rescued the vascular phenotype. These findings raised the possibility that TCF7L2 may play a causal role in acquisition and maintenance of vascular smooth muscle differentiation. This is an extremely relevant question as a SNP (single nucleotide polymorphism) in the gene encoding *TCF7L2* are considered the strongest genetic risk factors for T2DM by multiple GWAS and are associated with risk of CAD¹² and its severity¹³ in subjects with T2DM. This notion, however, is in sharp contrast with the previous findings that Wnt/TCF7L2 promotes cell cycle activation and proliferation during early embryogenesis and in adult stem cells.^{12,14,15} Additionally, whether the disease-associated *TCF7L2* common variants cause gain or loss of function has remained controversial.¹⁶ Thus, we embarked on comprehensive studies in mice that either globally overexpress or are haploinsufficient for TCF7L2 to (1) verify the causal role and (2) identify the mechanisms of action of TCF7L2 in regulation of VSMC plasticity, and (3) to establish that TCF7L2-driven VSMC differentiation plays a protective role to counteract the aberrant Wnt signaling and CAD because of the *LRP6^{R611C}* mutation. It should be emphasized that a germline *LRP6^{R611C}* variant promotes human CAD. *TCF7L2* GWAS risk alleles are also germline variants, and hence their associated traits may arise from their global

effects. Therefore, we used global overexpression or haploinsufficient mouse models to investigate the roles of TCF7L2 as a translationally relevant approach.

Materials and Methods

The data that support the findings of this study are available from the corresponding author on reasonable request.

Animals

Animal procedures were as per approved protocol of Yale University Institutional Animal Care and Use Committee. Mice overexpressing TCF7L2 under mouse TCF7L2 promoter (TCF7L2-bac mice) and TCF7L2 heterozygous knockout (TCF7L2^{+/-}) mice were obtained in collaboration from M. Nobrega's laboratory at The University of Chicago, Chicago, IL.¹⁷ These mice were then backcrossed to C57Bl6 mice (N>10). Wild-type (WT) littermates were used as controls. Generation of homozygous *LRP6^{R611C}* and *LRP6^{R611C}; LDLR^{-/-}* (low-density lipoprotein receptor knockout) mice were previously described.¹⁸ Generation of *LRP6^{R611C/R611C}*; TCF7L2-bac was done by crossing *LRP6^{R611C/R611C}* to C57Bl6 backcrossed TCF7L2-bac mice. *LRP6^{R611C/R611C}* homozygous mice are referred to as either *LRP6^{R611C}* in the text or *R611C* or *RC* mice in the figures. *LDLR^{-/-}* mice were obtained from Jackson Laboratory, Bar Harbor, ME. All mice were fed ad libitum and housed at constant ambient temperature in 12-hour light, 12-hour dark cycle. Both TCF7L2-bac male and female mice were studied. Male WT and TCF7L2^{+/-} were more predisposed to intimal hyperplasia, and, therefore, the results of their study are provided. Mice were examined at age 6 to 8 weeks. For high-cholesterol diet studies, 6 weeks old mice were fed high-cholesterol diet (40% fat, 1.25% cholesterol, and 0.5% cholic acid) ad libitum (Research Diets) for 4 or 6 weeks. All studies in animals were conducted in accordance with the National Institutes of Health Guidelines for the Care and Use of Laboratory Animals.

Chemicals and Antibodies

Protease inhibitor cocktail (P8340), phosphatase inhibitor cocktail (P2850), cycloheximide, MG132, and BrdU (bromodeoxyuridine) were purchased from Sigma-Aldrich. Cell lysis buffer (9803) and antibodies for β -actin, PDGFR β (platelet-derived growth factor receptor beta; 1:150), pPDGFR β (phosphorylated platelet-derived growth factor receptor beta; y751/y771, 1:1000), p-LRP6 (phosphorylated LRP6), and p53, Pp53(ser15, 1:3000), p38 (1:200), Pp38(Thr180/Tyr182, 1:1000), JNK (c-Jun N-terminal kinase; 1:500 mg/mL), Phospho-SAPK (stress-activated protein kinase)/JNK (1:1000, Thr183/Tyr185), cyclin D1, chromatin immunoprecipitation (ChIP) assay kit were all purchased from Cell Signaling Technology. DMEM, FBS, penicillin-streptomycin cocktail, Trypsin-EDTA solution, and TRIzol were purchased from GIBCO/Invitrogen; polyvinylidene fluoride (PVDF) membranes from Bio-Rad Laboratories; Antibodies for TCF7L2(sc-8631, 1:200, Santa Cruz Biotechnology, Inc), and protein A/G agarose gel were purchased from Santa Cruz Biotechnology. These TCF7L2 antibody has been previously validated by our group using RNA interference.¹⁹ Antibodies for α -SMA (alpha smooth muscle cell actin; 1 μ g/mL), and SM-MHC (smooth muscle cell myosin heavy chain; 0.4 μ g/mL), GATA6 (GATA-binding protein 6; rabbit, 1:200), p300 (1 μ g/mL), p16, were purchased from Abcam, GATA6 (goat) antibody was from Novus and CD31 antibody from BD PharMingen, and secondary fluorescence-tagged antibodies and propidium iodide from Invitrogen.

Immunofluorescence

Immunofluorescence staining was performed on 5- μ m frozen sections. All antibodies were diluted 1:200. No primary was used as control for all studies. Only previously validated antibodies were used. Fluorescence was measured using Nikon Eclipse80i or Zeiss 4 laser Confocal microscope using same laser output, gain, and offset for each set of antibodies tested. Images were quantified with Image J and adjusted for the area.

Western Blotting

Protein contents of the VSMC lysates were quantified by using Quant-iT Protein Assay Kit. Whole-cell lysates of primary VSMCs were separated by electrophoresis, transferred to PVDF membrane, and probed using target primary antibodies followed by appropriate HRP (horseradish peroxidase)-conjugated secondary antibodies. Blots were visualized using chemiluminescence reagents, imaged with Bio-Rad gel doc system, and quantified with Image J software.

VSMC Isolation and Culture

Isolation of aortic VSMCs was performed as previously described.²⁰ VSMCs were maintained in DMEM (4.5g/L glucose, glutamine, and 100 mg/L sodium pyruvate) supplemented with 20% FCS, 100 U mL⁻¹ penicillin, and 100 µg mL⁻¹ streptomycin. For phosphorylation studies, cells were starved for 3 hours in 0.2% FBS containing DMEM and were treated as follows: PDGF-BB (platelet-derived growth factor-BB) at 10 ng/mL for 15 minutes. For mRNA studies, the cells were starved overnight in DMEM containing 0.2% FBS and treated with PDGF-BB (10 ng/mL) for 24 hours. For protein half-life measurements, VSMC were pretreated with cycloheximide (CHX; 100 µg/mL) for 30 minutes and then incubated with or without PDGF-BB (10 ng/mL). Cells were harvested at 0-, 15-, and 30-minute intervals, cell lysates were subjected to Western blotting, and the GATA6 protein was quantified using Image J. For proteosomal degradation studies, VSMC were pretreated with MG132 (1 µM) for 1 hour followed by PDGF-BB (10 ng/mL) stimulation. The cell lysates were immunoprecipitated using GATA6 antibody, followed by Western blotting and probing with ubiquitin antibody.

ChIP Assay

Chromatin immunoprecipitation (ChIP) assay was performed according to the manufacturer's instructions (Cell Signaling SimpleChIP Enzymatic Chromatin IP Kit [Agarose Beads] number 9002). Briefly, the chromatin/DNA protein complexes were prepared from mouse aortic smooth muscle cells. Chemical crosslinking of DNA proteins was performed using 1% formaldehyde for 10 minutes at room temperature (RT) and followed by addition of glycine solution. Cells were scraped into cold PBS containing Halt cocktail proteinase inhibitor. The cell suspension was centrifuged, and the pellet was lysed, and nuclei were digested using micrococcal nuclease to digest DNA to a length of ≈200 to 1000 bp. Supernatant containing the digested chromatin was incubated with appropriate ChIP-grade TCF7L2 antibody (sc-8631; Santa Cruz Biotechnology) for immunoprecipitation overnight at 4°C with rotation, followed by ChIP-grade protein A/G agarose beads and incubation for 1 hour at 4°C with rotation. Anti-H3 antibody and RPL30 (ribosomal protein L30) primers provided in the kit were used as a positive control for assay technique and reagent integrity. The agarose resin was washed using buffers supplied with the kit. The eluted DNA was purified and analyzed by polymerase chain reaction (PCR) to determine the binding of TCF7L2 (TCF7L2 binding consensus: [A/T] [A/T] CAAAG) to Gata6 promoter. The following primers were used to amplify the binding region: forward 5'-GTCTTCGACGCCTAGCTTCA-3' and reverse 5'-CTAAATTTGGCGTCCTGGCTG-3'. Real-time PCR amplification was performed using iQ SYBR Green Supermix (Bio-Rad) and Eppendorf Mastercycler RealPlex2. Similar protocol used to amplify TCF/GATA6 binding site (cttggataa) in SMC-MHC intron2 with the primers 5'-TGCCTGGGTTTCATTCTGTG-3' and 5'-GGCCCTACCTCTCCATATC-3'.

Coimmunoprecipitation

For coimmunoprecipitation studies 1200 µg of total protein derived from WT VSMC lysate was divided in equal amount and then either used as input or immunoprecipitated with the IgG and TCF7L2 antibodies for overnight and protein A/G agarose beads at 4°C for 1 hour. Proteins were then solubilized in Laemmli sample loading buffer, applied SDS-PAGE, and transferred to a PVDF membrane and immunoblotted using different primary and HRP-conjugated

secondary antibodies. Enhanced chemiluminescence reagents were used to develop the blots.

Carotid Artery Guidewire Injury

The carotid artery guidewire injury was performed as previously described²¹ Three weeks postinjury, mice were euthanized and injured carotid arteries were excised from the arteriotomy site of external left carotid artery, including the internal left carotid artery and ≈1 cm of left common carotid artery. Similarly, right common carotids were harvested and used as uninjured controls. The arteries were embedded in OCT (optimal cutting temperature compound); serial tissue sections (5 µm) were obtained from left and right common carotid arteries, starting at the bifurcation (to external and internal carotids), and immunofluorescence, IHC, and morphometric analyses were performed. Neointima formation was measured in 10 sections (50 µm apart) using images obtained by a bright-field microscope and quantified using ImageJ software (National Institutes of Health).

In Vitro Scratch Wound-Healing Assay

Primary VSMC from WT and TCF7L2-bac aorta were grown to ≈70% to 80% confluency in 12 well plates in complete growth medium. The monolayer was scratched across the center of the well gently and slowly using tip of sterile 1 mL pipette tips and holding the tip perpendicular to the bottom of the well. After scratching, the wells were gently washed twice with culture medium to remove detached cells and filled with fresh culture medium. Microscope images were taken to note the initial scratch size, and the areas were marked. The cells were then left undisturbed for 18 hours and images were taken again. The gap distance covered was quantitatively evaluated as a percentage of the initial gap distance using Image J software.

In Vitro BrdU Staining

VSMC were grown to 70% to 80% confluency and starved overnight (DMEM with 0.2% FBS). Next cells were stimulated with or without PDGF-BB (10 ng/mL) followed by propidium iodide for nuclear staining for 24 hours. Then cells were pulsed with BrdU (10 µM/mL) for 4 hours at 37°C. BrdU solution was removed and washed with PBS (3×, 2 minutes each). The cells were fixed with 1 mL of 3.7% formaldehyde for 15 minutes at RT and washed with PBS (3×, 2 minutes each). Next, the cells were permeabilized with 1 mL of 0.1% Triton X-100 in PBS for 20 minutes at RT, followed by 1 mL of 1 N HCl for 20 minutes at RT, and finally neutralized with 0.1 M sodium borate buffer pH 8.5 for 30 minutes at RT and washed with 0.1% Triton X-100 in PBS (3×, 2 minutes each). The cells were incubated overnight with anti-BrdU antibody at 4°C, washed with 0.1% Triton X-100 in PBS (3×, 2 minutes each) followed by incubation with fluorescently labeled secondary antibody for 1 hour at RT. The cells were washed with PBS and imaged using fluorescence microscope.

Real-Time PCR

Total RNA was isolated from primary VSMC culture using TRIzol, and cDNA was generated using the High Capacity cDNA Reverse Transcription Kit (Applied Biosystems) according to the manufacturer's instructions. Real-time PCR amplification was performed using specific primers and iQ SYBR Green Supermix in Eppendorf Mastercycler RealPlex2. Reactions were performed in quadruple with a β-actin internal control. Relative quantification of mRNA levels was expressed as fold increase relative to the control. The following mouse primer sequences were used for quantitative real-time-PCR:

- Gata6 Forward: ATGCGGTCTCTACAGCAAGATGA
- Gata6 Reverse: CGCCATAAGGTAGTGGTTGTGG
- TCF7L2 Forward: CGCTGACAGTCAACGCATCTATG
- TCF7L2 Reverse: GGAGGATTCCTGCTTGACTGTC
- SM-MHC Forward: GCAACTACAGGCTGAGAGGAAG
- SM-MHC Reverse: TCAGCCGTGACCTTCTCTAGCT
- βactin Forward: CATTGCTGACAGGATGCAGAAGG
- βactin Reverse: TGCTGGAAGGTGGACAGTGAGG

Statistical Analyses

In all experiments, at least 7 mice were used per group unless stated differently in the text or legend. Guidewire injury studies were done using at least 10 mice per group. All in vitro studies were performed in 3 independent experiments in triplicate. Fluorescence and area measurements were done using Image J software (National Institutes of Health). Preparation of graphs and all statistical analyses of results by 2-tailed Student *t* test were performed using for pairwise comparison and a 1-way ANOVA (SigmaPlot) for multiple comparison using GraphPad Prism 7 Project software (GraphPad) and testing for equal variance. For all experiment, normal distribution was tested by D'Agostino and Pearson omnibus K2 normality test. A few data that failed the normality test were analyzed by the Mann-Whitney *U* test. Bonferroni corrected $P < 0.05$ was considered as significant. Data are presented as mean \pm SD.

Results

TCF7L2 Expression Modulates Postinjury Intimal Hyperplasia

Vascular injury results in VSMC loss of differentiation and their subsequent proliferation.²² We first examined the TCF7L2 protein levels in WT mice with or without carotid artery wire injury by using immunofluorescent staining, using TCF7L2-specific antibody. VSMCs in WT carotid artery stained robustly for TCF7L2 at baseline, which was reduced 3 weeks after wire injury (Figure 1A, fluorescence/area before and after injury is shown).

To examine the relationship between TCF7L2 levels and VSMC phenotype, we backcrossed BALB/c humanized TCF7L2 overexpressing BAC (bacterial artificial chromosome) transgenic mice (transgenic mouse lines harboring engineered enhancer-trapped human bac RP11-466I19 spanning the entire T2DM-associated interval recombined with a full-length mouse *Tcf7l2* cDNA) and heterozygote knockout mice (generated using zinc finger nuclease technology targeted to the constitutive exon 11 encoding the High Mobility Group box DNA-binding domain of the protein) with C57BL6 mice, until we generated N10 (10 generation) heterozygote overexpressing (TCF7L2-bac) and heterozygous knockout (*TCF7L2*^{+/-}) mice. *TCF7L2*^{-/-} mice were born in Mendelian ratio but died within \approx 24 hours of birth because of feeding problem from lack of gut development as previously reported.²³ The reason for the backcrossing was (1) LRP6 mice used in the rescue experiments are of C57BL6 background and (2) BALB/c mice are resistant to atherosclerosis.²⁴

Uninjured TCF7L2-bac mice exhibited >1.7-fold higher levels of mostly nuclear TCF7L2 in VSMCs compared with WT mice by immunofluorescence staining (Figure 1B). We then examined the effect of TCF7L2 expression in response to mechanical injury on neointima formation using immunofluorescence staining and confocal microscopy. As expected, the injury resulted in reduced TCF7L2 in WT mice. TCF7L2 levels were, however, 2.5-fold higher in TCF7L2-bac mice versus WT littermates after the wire injury (Figure 1B). Strikingly, TCF7L2-bac male and female mice were both protected against neointima formation postinjury compared with sex-matched WT littermates (Figure 1C). Reduced TCF7L2 immunofluorescence staining after carotid injury in WT mice was associated with marked reduction in the level of contractile proteins SM-MHC (Figure 1D) and α -SMA (Figure 1E), indicating loss of differentiation of VSMC. Conversely, the levels of contractile proteins after the injury were by far higher in TCF7L2-bac versus WT mice carotids (Figure 1D and 1E).

We then compared the effect of carotid wire injury on neointima formation in *TCF7L2*^{+/-} mice compared with their WT littermates. TCF7L2 protein levels (aka TCF4) were reduced by about 50% in *TCF7L2*^{+/-} mice (Figure 1A in the [online-only Data Supplement](#)). In contrast to TCF7L2-bac mice, *TCF7L2*^{+/-} mice showed greater neointima formation and marked reduction of TCF7L2 levels by immunofluorescence staining postinjury compared with WT littermates (Figure 2B and 2C). Accordingly, the fall in TCF7L2 expression after injury in *TCF7L2*^{+/-} mice was accompanied by a decline in the levels of contractile proteins SM-MHC and α -SMA in VSMC assessed by immunofluorescence staining (Figure 2D and 2E).

TCF7L2 Abrogated VSMC Migration and PDGF-Stimulated Proliferation In Vitro

Intimal hyperplasia in response to injury is associated with VSMC migration and proliferation. To demonstrate that the protection against intimal hyperplasia in TCF7L2-bac mice is because of the effect of the VSMCs, we isolated WT and TCF7L2-bac aortic VSMCs and performed migration and proliferation assays. In vitro scratch assay showed that TCF7L2-bac aortic VSMC cultured with FBS migrated considerably slower than WT aortic VSMC (Figure 3A). PDGF signaling has an established role in triggering VSMC proliferation.^{25,26} A proliferation assay with and without PDGF-BB stimulation for 24 hours was performed on isolated aortic WT, TCF7L2-bac and *TCF7L2*^{+/-} VSMC. TCF7L2-bac aortic VSMC showed lower BrdU incorporation and cell count after PDGF-BB stimulation compared with WT aortic VSMC (Figure 3B, quantifications shown underneath). *TCF7L2*^{+/-} VSMC had expectedly greater BrdU incorporation and cell number compared with WT VSMC after PDGF-BB stimulation (Figure 3C, quantifications shown underneath). Taken together, these data suggest that TCF7L2 inhibits cell migration and PDGF-dependent cell proliferation.

TCF7L2 Regulates Cell Cycle Checkpoints

TP53 (p53) and p16 have been implicated in preventing entry into mitosis as part of cell cycle checkpoint mechanisms. p16 is a downstream target of p53^{27,28} and is also implicated in G2 arrest during cellular senescence.²⁹ We examined P-p53 (phosphorylated TP-53) and p16 levels in WT, *TCF7L2*^{+/-}, and TCF7L2-bac VSMC by immunohistochemistry. Both cell cycle inhibitors were downregulated in WT VSMCs but not in TCF7L2-bac VSMC after vascular injury compared with baseline (Figure 3D and 3E, quantification underneath Figure 3D). Accordingly, immunofluorescent analysis showed lower P-p53 levels in *TCF7L2*^{+/-} versus WT VSMCs (Figure 1B in the [online-only Data Supplement](#)). Western blot analysis confirmed higher baseline p-p53 and p16 protein levels in TCF7L2-bac and lower levels of these proteins in *TCF7L2*^{+/-} VSMC compared with their WT littermates (Figure 3F, quantifications underneath the figure).

It has been previously shown that TCF7L2 binds the p53 promoter and transcriptionally regulates this gene.³⁰ We, therefore, examined the p53 mRNA levels, which were dramatically lower in *TCF7L2*^{+/-} and higher in TCF7L2-bac compared with WT VSMCs (Figure 3G). Notably, this effect of TCF7L2 in VSMCs is in contrast with its effect in proliferating pancreatic beta cells in which TCF7L2 represses p53 expression.³⁰

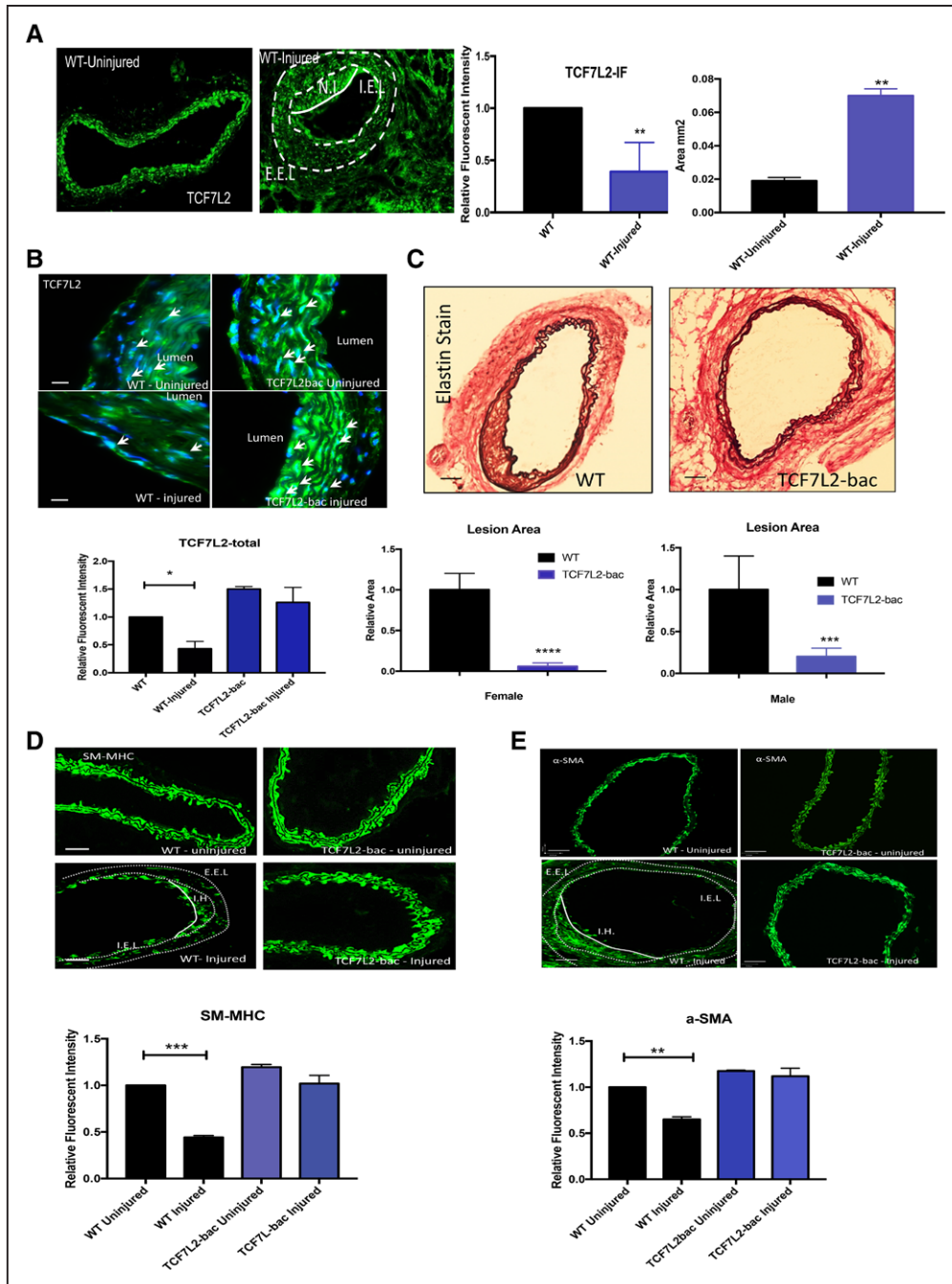


Figure 1. A–E, Response to mechanical injury in TCF7L2 (transcription factor 7-like 2) overexpressing mice. **A,** Immunofluorescence (IF) staining of TCF7L2 in wild-type (WT) mouse carotid at baseline and post guidewire injury (relative fluorescent intensities/area and the tunica media (M) area are shown next to the figure). **B,** TCF7L2 IF intensity in heterozygote overexpressing (TCF7L2-bac) and WT mice before and after injury (relative fluorescent intensities shown underneath). **C,** Neointima (NI) formation and EVG (elastic tissue fibers-Verhoeff’s Van Gieson) staining in carotid arteries of WT and TCF7L2-bac mice post-guidewire injury. Quantifications of NI for both female and male WT and TCF7L2-bac mice postcarotid guidewire injury are shown underneath corresponding figures. The quantification is done by the ratio of intima/M surface area. **D** and **E,** Immunofluorescent assessment of SM-MHC (smooth muscle cell myosin heavy chain) and α -SMA (alpha smooth muscle cell actin; both in green) in carotids of TCF7L2-bac, and WT mice, before and after guidewire injury. The relative fluorescent intensities shown underneath. The yellow dotted lined in (A) demarcate the NI. *, **, ***, ****Significance with $P < 0.05$, < 0.01 , < 0.001 , and < 0.0001 , respectively, by ANOVA. Quantifications of IF intensity are average of 8 sections per mice (7 mice in each group). Scale bars, 16 μ m. EEL indicates external elastic lamina; IEL, internal elastic lamina; and IH, intimal hyperplasia.

Association Between TCF7L2 and GATA6 in VSMC
 GATA6 has been recognized as a key regulator of VSMC differentiation.³¹ This transcription factor promotes VSMC differentiation by stimulating the expression of contractile proteins and inhibiting cell cycle progression.³² The shared

function of TCF7L2 and GATA6 with respect to promoting the expression of contractile proteins prompted an examination into possible interaction between the 2 proteins. We compared the GATA6 protein levels of WT, *TCF7L2*^{+/-}, and TCF7L2-bac mice carotid arteries before and after wire

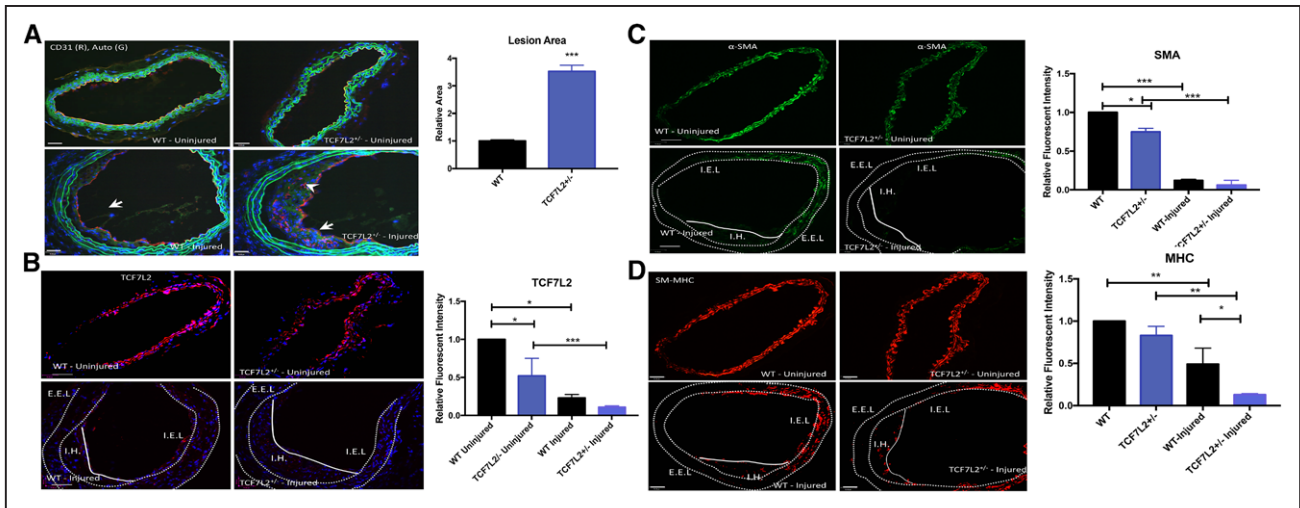


Figure 2. Response to mechanical injury in *TCF7L2^{+/-}* mice. **A**, Neointima formation and its quantification in carotid arteries of wild-type (WT) and *TCF7L2^{+/-}* mice postguidewire injury. **B**, Immunofluorescence (IF) staining of carotid for TCF7L2 (transcription factor 7-like 2) in uninjured and injured (3 wk after wire injury) *TCF7L2^{+/-}* and WT mice. **C–D**, Immunofluorescent assessment of T α -SMA (alpha smooth muscle cell actin) and SM-MHC (smooth muscle cell myosin heavy chain) in carotids of *TCF7L2^{+/-}* and WT mice, before and after guidewire injury. Quantifications are shown next to corresponding figures. *, **, ***Significance with $P < 0.05$, < 0.01 , and < 0.001 , respectively, by ANOVA. Quantifications of IF intensity are average of 8 sections per mice (7 mice in each group). Scale bars, 16 μ m. The dotted lines circumscribe the neointima. EEL indicates external elastic lamina; IEL, internal elastic lamina; and IH, intimal hyperplasia.

injury by immunofluorescence staining. Baseline GATA6 levels were modestly higher in *TCF7L2*-bac compared with WT mice VSMCs (Figure 4A). GATA6 levels were drastically reduced after injury in WT mice and *TCF7L2^{+/-}* mice (Figure 4C in the [online-only Data Supplement](#)), but GATA6 levels in *TCF7L2*-bac mice postinjury were considerably higher compared with WT mice (Figure 4A). We then costained for TCF7L2 and GATA6 and examined their subcellular localization in VSMCs of the tunica media of WT mice with and without carotid artery injury using confocal microscopy. The results showed that in quiescent arteries, TCF7L2 and GATA6 localize within the nucleus in VSMC, but their expression levels drastically dropped after the injury, and with the nuclear exclusion of TCF7L2, they no longer colocalized (Figure 4B and Figure 4D in the [online-only Data Supplement](#)).

These findings raised the question of whether TCF7L2 regulates GATA6 expression. GATA6 transcripts are downregulated in response to mitogens.³³ PDGF is a major mitogen that has an established role in inducing loss of differentiation and proliferation of VSMCs postinjury^{34,35} and is inhibited by Wnt activation.^{11,36} To examine if TCF7L2 transcriptionally regulates GATA6, we treated WT and *TCF7L2*-bac VSMC with or without PDGF-BB for 24 hours and measured the GATA6 and SM-MHC mRNA expression levels by quantitative real-time-PCR. Baseline GATA6 mRNA levels were higher in *TCF7L2*-bac versus WT VSMC. The mRNA expression levels of TCF7L2 and GATA6 were both dramatically reduced after PDGF-BB stimulation in WT VSMC. As anticipated, there was a concurrent decline in SM-MHC (aka *MYH11*) mRNA expression (Figure 4C). Notably, PDGF-induced repression of TCF7L2, GATA6, and SM-MHC mRNA levels was significantly attenuated in *TCF7L2*-bac aortic VSMC (Figure 4C).

The GATA6 promoter has multiple (T-C-A-A-A-G or C-T-T-T-G-A) motifs as putative sites for TCF7L2 binding. We, therefore, performed a ChIP assay to examine TCF7L2 binding to the GATA6 promoter using ChIP-grade TCF7L2 antibody³⁷

for pulldown and amplifying the region of the mouse GATA6 promoter bearing the putative TCF7L2 binding sites using specific primers. The assay revealed specific binding of TCF7L2 to the GATA6 promoter (Figure 4D). GATA6 promoter binding by TCF7L2 was expectedly stronger in *TCF7L2*-bac versus WT VSMC (Figure 4D). We then compared GATA6 mRNA levels between WT and *TCF7L2^{+/-}* carotid artery lysate before and after injury. The GATA6 mRNA levels were not different between the WT and *TCF7L2^{+/-}* mice carotids at baseline. The GATA6 mRNA and protein levels assayed by immunofluorescence were dramatically reduced after injury in both WT and *TCF7L2^{+/-}* mice carotids (Figure 4E). These findings suggested that TCF7L2 protects VSMCs against PDGF-mediated transcriptional inhibition of GATA6 but is not required to maintain it under normal condition. Importantly, the effects of TCF7L2 on GATA6 mRNA levels were modest and did not entirely account for the more robust effects observed at the protein level in vivo. This prompted an investigation into post-transcriptional regulation of GATA6 by TCF7L2.

TCF7L2 Is Protective Against PDGF-Dependent Turnover of GATA6

Activation of the PDGF downstream effector JNK has been shown to promote the proteolytic degradation of GATA6.³⁸ JNK activator anisomycin has been shown to efficiently export nuclear GATA6 into the cytoplasm and initiates its degradation by proteasomes, and this effect is inhibited by JNK inhibitor SP600125. We had previously shown that LRP6/Wnt inhibits PDGF signaling by promoting PDGFR β ubiquitination and diminishing JNK signaling. Subsequent in vitro and in vivo investigations had found that impaired Wnt signaling results in increased activation of PDGF signaling,¹¹ which is normalized by systemic Wnt3a administration in vivo and by TCF7L2 overexpression in VSMCs in vitro.¹¹ Thus, we hypothesized that TCF7L2 may stabilize GATA6 protein by inhibiting PDGF/JNK activation. To examine this

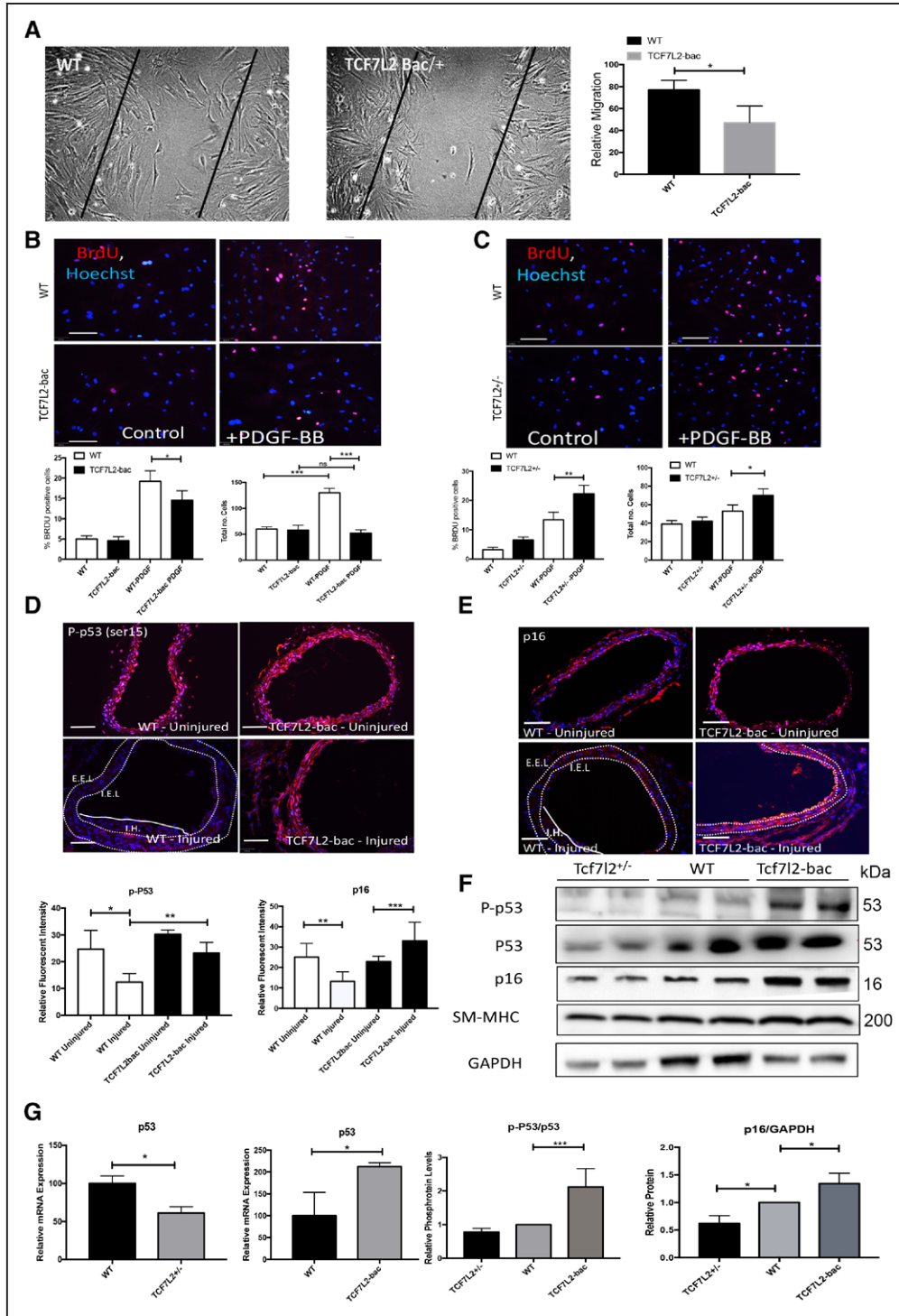


Figure 3. Cell migration and proliferation in TCF7L2 (transcription factor 7-like 2)-bac (mice overexpressing TCF7L2) and TCF7L2^{+/-}-mice vascular Smooth muscle cell (VSMCs). **A**, In vitro scratch assay demonstrating slower TCF7L2-bac VSMC migration as compared to wild-type (WT) VSMC (the quantification is shown next to the figure). Area in between the solid black lines indicates the scratch in the VSMC culture. Relative migration in wound-healing assay was assessed as a percentage of the initial gap filled with cells. **B** and **C**, Proliferation assay with BrdU (bromodeoxyuridine) incorporation and cell count analysis with and without PDGF-BB (platelet-derived growth factor-BB) stimulation for 24 h in TCF7L2-bac and TCF7L2^{-/-} VSMC, respectively (quantification shown left underneath). **D** and **E**, immunofluorescence staining of carotid artery for P-p53 (phosphorylated TP53) and p16 protein in WT and TCF7L2-bac mice before and after injury (quantification shown underneath **D**). **F**, Protein levels of P-p53, p53, p16, and SM-MHC (smooth muscle cell myosin heavy chain) in WT, TCF7L2-bac and TCF7L2^{-/-} mice VSMCs by Western blot analysis (quantification shown below, multiple comparison done by ANOVA). **G**, Relative mRNA expression of p53 in TCF7L2^{-/-} and TCF7L2-bac mice. *, **, and ***Significance with $P < 0.05$, < 0.01 , < 0.005 for comparison of the transgenic with the WT mice, respectively. Dotted lines and N denote neointima. Quantification are average of 4 experiments per condition. Scale bar, 16 μ m. EEL indicates external elastic lamina; IEL, internal elastic lamina; and IH, intimal hyperplasia.

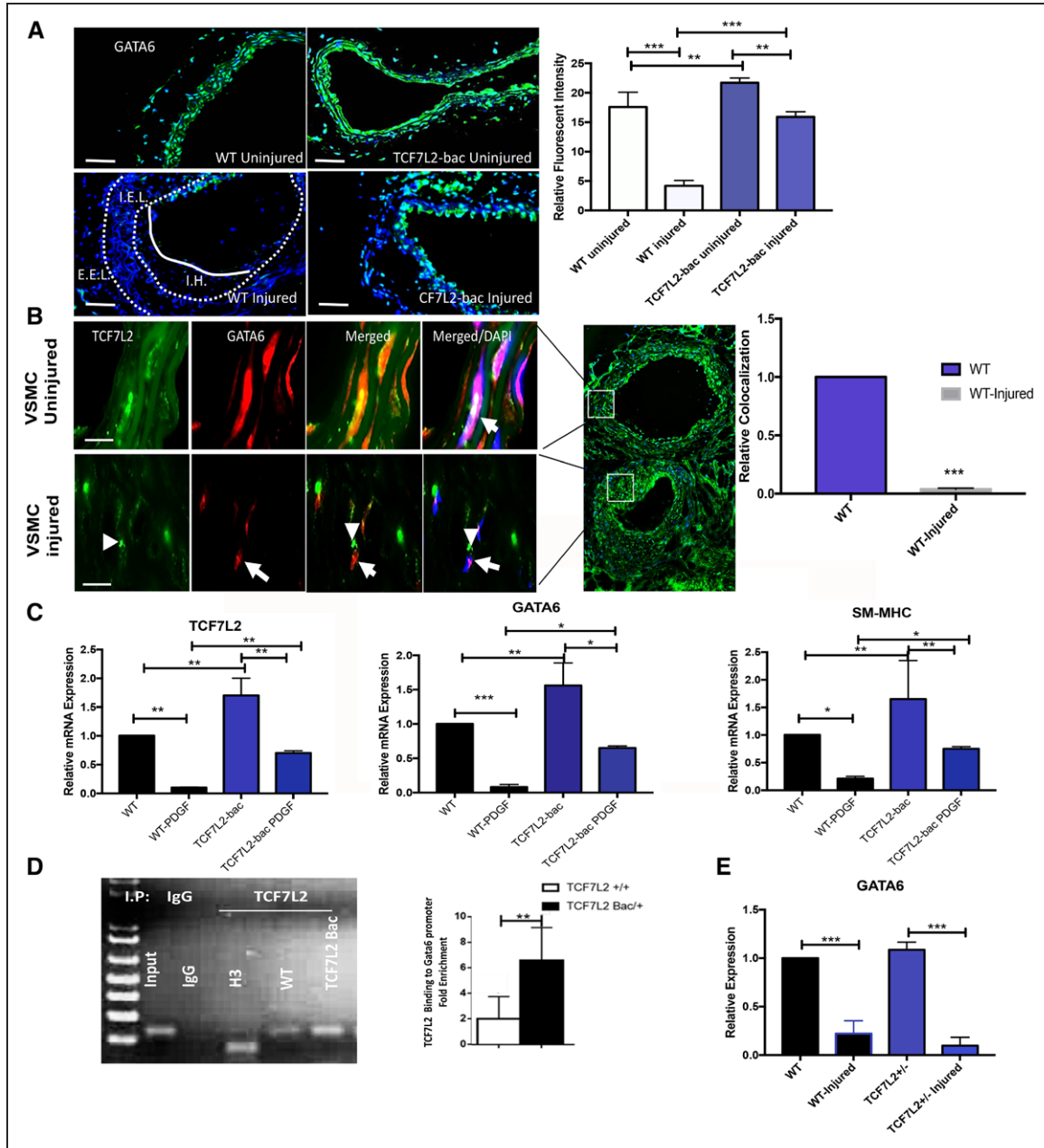


Figure 4. GATA6 (GATA-binding protein 6) expression, localization, and transcriptional regulation. **A**, Immunofluorescence (IF) staining of GATA6 in wild-type (WT) and TCF7L2 (transcription factor 7-like 2)-bac mice (mice overexpressing TCF7L2) carotids, before and after guidewire injury (quantification shown next to the figure). **B**, Subcellular localization of TCF7L2 and GATA6 in tunica media of injured and uninjured carotid artery of WT mice. Colocalization of TCF7L2 and GATA6 in the nucleus and its loss after injury, arrows and arrowheads show GATA6 and TCF7L2, respectively. Nuclei are stained with DAPI (4',6-diamidino-2-phenylindole). **C**, TCF7L2, GATA6, and SM-MHC (smooth muscle cell myosin heavy chain) mRNA expression in TCF7L2-bac vs WT vascular smooth muscle cell (VSMC), with and without PDGF-BB (platelet-derived growth factor-BB) stimulation. **D**, Chromatin immunoprecipitation assay demonstrating TCF7L2 binding to GATA6 promoter in WT and TCF7L2-bac VSMCs; its quantification shown next to the figure. **E**, GATA6 mRNA expression in WT and TCF7L2^{-/-} mice aortic lysate, before and after guidewire injury. *, **, and ***Significance with $P < 0.05$, < 0.01 , and < 0.001 by ANOVA for multiple comparisons, respectively. Quantifications of IF intensity are average of 8 sections per mice (7 mice in each group). Scale bars, 16 μ m. EEL indicates external elastic lamina; IEL, internal elastic lamina; and IH, intimal hyperplasia.

hypothesis, we measured GATA6 protein levels in VSMC of WT and TCF7L2-bac mice with and without PDGF-BB treatment after inhibiting protein synthesis by cycloheximide. The analysis showed greater GATA6 protein levels in TCF7L2-bac versus WT VSMCs. PDGF-BB dramatically reduced GATA6 protein levels in WT VSMC within 15 minutes of stimulation (Figure 5A), whereas GATA6 was only marginally reduced in

TCF7L2-bac and after 30 minutes of stimulation. This robust and reproducible finding implicated TCF7L2 in stabilization of GATA6 against PDGF-BB.

We then examined the effect of TCF7L2 overexpression on PDGF signaling in WT versus TCF7L2-bac VSMCs stimulated with PDGF-BB. There was significantly lower total and phosphorylated PDGFR β in TCF7L2-bac versus WT VSMC

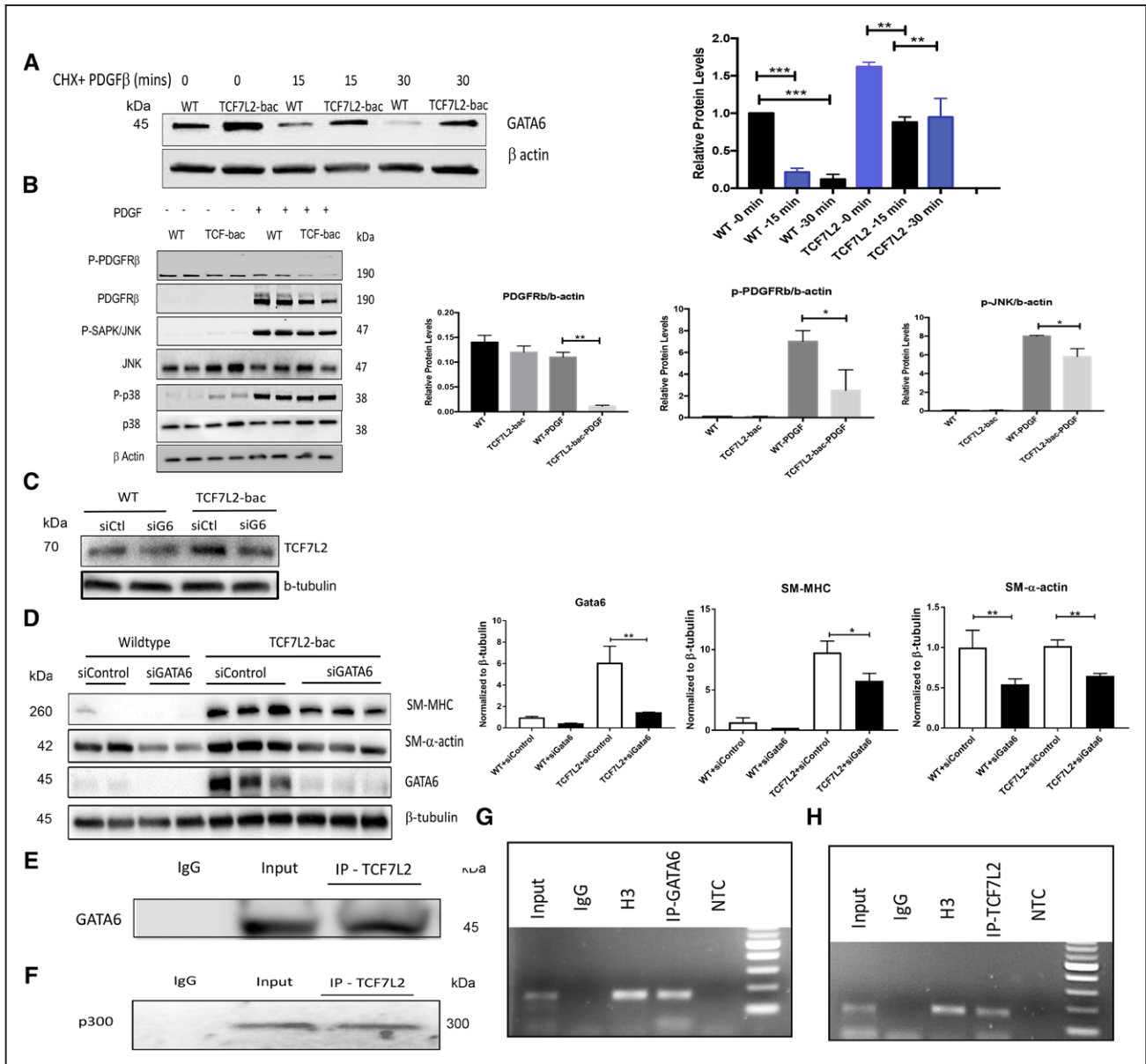


Figure 5. TCF7L2 (transcription factor 7-like 2) stabilizes GATA6 (GATA-binding protein 6) against PDGF (platelet-derived growth factor), forms a complex with it and jointly regulates SM-MHC (smooth muscle cell myosin heavy chain) transcription. **A**, Time course of GATA6 protein levels after PDGF-BB stimulation in CHX pretreated wild-type (WT) and TCF7L2-bac (TCF7L2 overexpressing) vascular smooth muscle cells (VSMC) by Western blot, quantifications shown next to the figure. **B**, PDGFRβ (platelet-derived growth factor receptor beta) expression and phosphorylation and activation of its downstream effectors, JNK/SAPK (c-Jun N-terminal kinases/stress-activated kinases) and ERK1/2 (extracellular-signal-regulated kinase 1/2) and in WT and TCF7L2-bac VSMC on PDGF-BB stimulation, quantifications shown next to the figure. **C**, GATA6 knockdown by siRNA and **(D)** its effect on the protein levels of SM-MHC and SMA (alpha smooth muscle actin) in WT and TCF7L2-bac VSMC, quantifications shown next to the figure. **E**, Immunoprecipitation of TCF7L2 and GATA6 in WT and TCF7L2-bac VSMC lysates, TCF7L2-specific antibody was used for pulldown, followed by Western blot analysis for GATA6. **F**, Immunoprecipitation of TCF7L2 and p300 in WT VSMC lysates; TCF7L2-specific antibody was used for pulldown, followed by Western blot analysis for p300. **G** and **H**, Chromatin immunoprecipitation (ChIP) assay demonstrating bindings of TCF7L2 and GATA6 to SM-MHC promoter in VSMC (WT) using ChIP-grade TCF7L2-specific and GATA6-specific antibody, respectively. IgG is used as a negative and input as a positive control. *, **, and ***Significance with $P < 0.05$, < 0.01 , < 0.001 for multiple comparison in 5A by ANOVA and pairwise comparisons between WT and TCF7L2-bac for each condition using *T* test in all other figures, respectively. Quantification are average of 4 experiments per mice (7 mice in each group). CHX indicates cycloheximide; NTC, nontemplate control; p-PDGFR, phosphorylated PDGFR; p-JNK, phosphorylated JNK; siControl, scrambled siRNA (small interfering ribonucleic acid); and siGATA, siRNA against GATA6.

after PDGF-BB stimulation (Figure 5B). Consequently, there was reduced activation of its PDGF downstream effector JNK/SAPK (and p38) in TCF7L2-bac compared with WT VSMC (Figure 5B). These findings identify TCF7L2 inhibition of PDGF/JNK as one of the mechanisms for GATA6 stabilization.

TCF7L2 and GATA6 Complex Formation and Binding of SM-MHC Promoter

To verify if GATA6 mediates the TCF7L2 regulation of SM-MHC, we knocked down GATA6 in WT and TCF7L2-bac VSMCs by siRNA. GATA6 protein levels were markedly increased in the TCF7L2-bac and were knocked down by

about 80% by GATA6 siRNA (small interfering ribonucleic acid; Figure 5D). Consequently, SM-MHC protein levels were significantly reduced in TCF7L2-bac VSMCs compared with control siRNA (siControl, quantifications are shown next to the figure; Figure 5D). SM-MHC protein levels continued to be higher in TCF7L2-bac compared with WT cells, either due to incomplete knockdown of GATA6 or GATA6-independent regulation of SM-MHC by TCF7L2. Taken together, these findings suggested that TCF7L2 regulates SM-MHC via GATA6-dependent and potentially GATA6-independent mechanisms.

Given that TCF7L2 and GATA6 colocalize in the nucleus, have similar functions and exhibit similar responses to perturbations, the possibility that they may have a combinatorial effect on SM-MHC transcription was raised. Thus, we examined if TCF7L2 and GATA6 form a complex. A pull-down assay using TCF7L2-specific antibody followed by Western blot analysis using GATA6-specific antibody showed that TCF7L2 and GATA6 coimmunoprecipitate (Figure 5E). GATA6 has been shown to form a complex with p300 to regulate transcription of SM-MHC in a combinatorial fashion.³¹ An immunoprecipitation assay in VSMC showed that TCF7L2 also forms a complex with p300 (Figure 5F), suggesting a potential combinatorial interaction between GATA6, TCF7L2, and p300. We then performed an in-silico screening of genes encoding VSMC contractile proteins for putative consensus TCF7L2 binding motifs. Interestingly, several consensus binding sequences for TCF7L2 and GATA6 were found either in tandem or overlapping by 1 or 2 nucleotides. We focused on one such consensus (CTTTGATAA) that lies between untranslated exon 1 and exon 2 in the open chromatin region of *SM-MHC* gene as defined by DNase I hypersensitivity (Figure IIA in the [online-only Data Supplement](#), shown in the ascending aorta). We performed 2 independent ChIP assays using ChIP-grade antibodies specific for TCF7L2 or GATA6. The assays revealed that both proteins bind to a region containing this motif in mouse VSMC (Figure 5G and 5H). Overall, these findings indicate that TCF7L2 and GATA6 are both implicated in transcriptional regulation of SM-MHC gene and suggest a potential combinatorial interaction between the two in this process.

TCF7L2 Overexpression Rescues Postcarotid Injury Neointima Formation in *LRP6^{R611C}* Mice

We had previously shown that impaired LRP6 activity in *LRP6* mutant mice (*LRP6^{R611C}*) leads to enhanced noncanonical Wnt signaling and a subsequent increase in TCF7L2 turnover and reduced SM-MHC protein levels.¹¹ These cascades of events culminate in excessive intimal hyperplasia. To (1) establish a causal link between reduced TCF7L2 expression, VSMC dedifferentiation, and intimal hyperplasia and (2) demonstrate that TCF7L2-mediated VSMC differentiation and reduced proliferation is protective against intimal hyperplasia, a rescue experiment in *LRP6^{R611C}* mice was performed. We crossbred TCF7L2-bac onto *LRP6^{R611C}* mice and examined the effect of TCF7L2 overexpression on GATA6 levels and SM-MHC in carotid injury neointima formation. Compared with *LRP6^{R611C}* mice, *LRP6^{R611C}; TCF7L2-bac* mice exhibited higher TCF7L2 and GATA6 protein levels (Figure 6A, quantification underneath). We then examined whether TCF7L2 overexpression rescues carotid artery intimal hyperplasia after guidewire injury in *LRP6^{R611C}* mice. As

expected, TCF7L2 overexpression had protective effects against neointima formation in *LRP6^{R611C}*; TCF7L2-bac (Figure 6B, quantifications underneath). Furthermore, increased GATA6 levels in *LRP6^{R611C}*; TCF7L2-bac mice were associated with increased staining for SM-MHC compared with *LRP6^{R611C}* mice. Of note, the overexpression of TCF7L2 was also associated with increased levels of activated (phosphorylated) LRP6 phosphorylation (Figure 6B), which may suggest a positive feedback mechanism. The exact molecular mechanisms of this phosphorylation has not been elaborated.³⁹

TCF7L2 Expression in Atherosclerosis Model

We had previously shown that TCF7L2 is highly expressed in VSMCs.¹¹ However, its significance in atherosclerosis process had not been studied. We assessed TCF7L2 protein levels in the aortic root and coronary arteries of *LDLR^{-/-}* versus WT mice. Strikingly, TCF7L2 levels were also lower in the aortic root and coronary arteries of *LDLR^{-/-}* versus WT mice on high-fat diet (Figure 6C). These changes were also associated with reduced α -SMA levels in VSMC of *LDLR^{-/-}* mice compared with WT mice (Figure 6D).

TCF7L2 Risk Alleles Are Associated With Reduced Gene Expression in the Aorta

Common variants of TCF7L2 gene have been the strongest signal in GWAS of T2DM and age-related endophenotypes¹⁴ ($P < 8 \times 10^{-17}$) and are associated with risk of CAD¹² and its severity¹³ in subjects with T2DM. Because of the small effect size of these variants, however, the disease mechanisms have remained unclear. Delineating TCF7L2 function in regulation of VSMCs is critical for understanding the pathogenesis of arterial disease in T2DM. Analyses of GTEX (Genotype-Tissue Expression) project data revealed that DM2 and CAD-associated TCF7L2 minor alleles (ie, rs4506565; Figure IIB in the [online-only Data Supplement](#)) are in disequilibrium with the expression QTLs (quantitative trait locus) variants of TCF7L2 (ie, rs6585200 and rs6585201, $P < 1.5 \times 10^{-10}$, NES (number of empty spikelets per panicle) -0.31 ; Figure IIC in the [online-only Data Supplement](#)). Based on Genotype-Tissue Expression data, QTLs variants of TCF7L2 are most significantly associated with reduced TCF7L2 expression in the aorta and tibial artery (Figure IID and IIE in the [online-only Data Supplement](#), <http://www.gtexportal.org/home/eqtls/byGene?geneId=tcf7l2&tissueName=All>). Taken together, these findings in human atherosclerosis and *LDLR^{-/-}* mice indicate the relevance of our findings in the TCF7L2 mouse models and the significance of TCF7L2 expression levels for normal arterial function.

Discussion

Mutations in Wnt-coreceptor LRP6-regulated proteins have been associated with CAD.⁴⁰ The causality of LRP6 mutation has been established in a mouse model of human mutation that exhibits severe obstructive CAD, characterized by excessive proliferation of poorly differentiated VSMCs.¹¹ The roles of downstream effectors of Wnt/LRP6 in regulation of vascular plasticity are poorly understood and, in some cases, controversial. Here, we examine in detail the role of TCF7L2 in VSMC and identify it as a key regulator of VSMC differentiation.

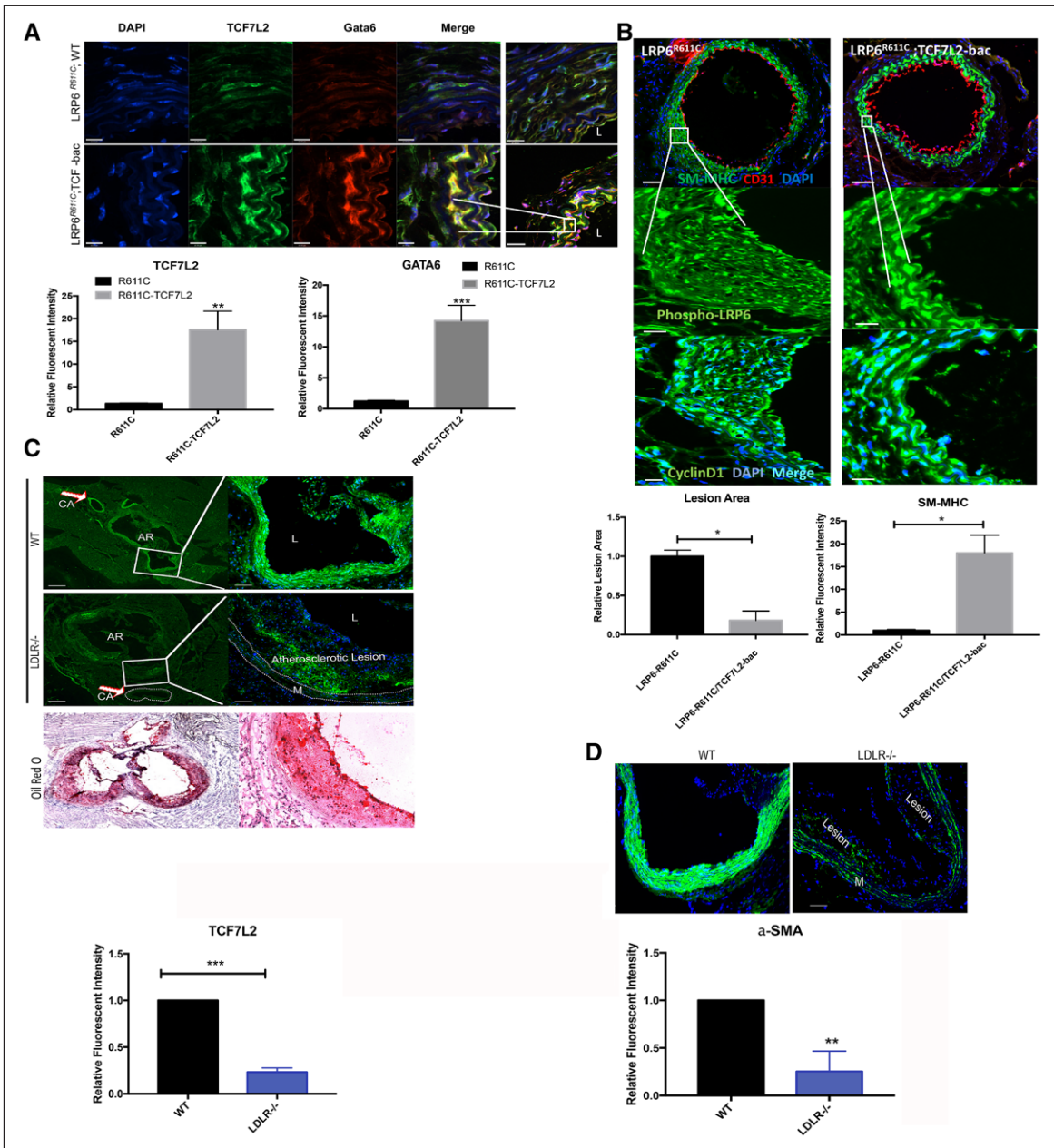


Figure 6. TCF7L2 (transcription factor 7-like 2) overexpression rescues postcarotid injury neointima formation in *LRP6*^{R611C} mice. **A**, Relative intensity of TCF7L2 and GATA6 (GATA-binding protein 6) in *LRP6*^{R611C} and *LRP6*^{R611C}; TCF7L2-bac (TCF7L2 overexpressing) mice carotids by immunofluorescence (IF). Magnification (×100) is shown on the **right** and the area magnified by 5 folds shown on the **left**. **B**, Neointima formation (**top row**) and IF staining of carotid artery post injury for SM-MHC (smooth muscle cell myosin heavy chain), CD31 (**top row**), p-LRP6 (phosphorylated LDLR-related protein 6; second row) and cyclinD1 (third row) in *LRP6*^{R611C} vs *LRP6*^{R611C}; TCF7L2-bac mice (nuclei are stained with DAPI [4',6-diamidino-2-phenylindole]); the quantifications for the relative lesion area and SM-MHC are shown. **C**, TCF7L2 and **(D)** α-SMA (alpha smooth muscle cell actin) IF staining in the aortic roots of the LDLR^{-/-} (low-density lipoprotein receptor knockout) vs wild-type (WT) mice on high-fat diet. Oil Red O staining shown for better visualization of the lesions in the LDLR^{-/-} mice. The boxes denote the sections of aortic roots that are enlarged. The quantifications are shown underneath corresponding figures. *, **, and ***Significance with *P* <0.05, <0.01, <0.001 by pairwise comparison respectively. Scale bars, 16 μm. AR indicates aortic root; CA, coronary artery; L, lumen; and M, media.

Except for in few proliferating tissues, Wnt/β catenin signaling is inactive in most normal adult organs.¹⁰ It has been shown that in the Wnt-inactive state TCF7L2 acts as a transcription suppressor by binding HDACs (histone deacetylases) and other transcription suppressors.⁴¹ In this article, we show that TCF7L2 actively promotes VSMC differentiation by upregulating GATA6, a transcription factor that is highly expressed in VSMC, and promotes their differentiation. TCF7L2 achieves this function by transcriptional and

posttranscriptional regulation of GATA6. Both TCF7L2 and GATA6 bind p300, which is a histone-acetyl transferase required for the GATA6 transcriptional activation of SM-MHC.³¹

Vascular injury and ensuing intimal hyperplasia are associated with mitogen secretion and downregulation of GATA6 transcripts in VSMCs.³³ Activation of PDGF as the most potent mitogen and its downstream signaling molecule JNK has been shown to induce proteosomal degradation of GATA6.³⁸ We show here that vascular mechanical injury or perturbations that

result from loss of LDLR or LRP6 mutation similarly cause downregulation of TCF7L2 in VSMC. In this context, the link between TCF7L2 and GATA6 is apparent in mice overexpressing TCF7L2, which are resistant against vascular injury by stabilizing GATA6 and maintaining the differentiated state of VSMCs. TCF7L2 and GATA6 jointly bind an open chromatin region in the MYH11 (AKA. SMC-MHC) promoter and induce SM-MHC transcription. Based on RNA-interference studies GATA6 seems as necessary but not sufficient for upregulation of SM-MHC involved in cellular differentiation. This raises the possibility of other combinatorial interactions between TCF7L2 and other transcription factors that are yet to be discovered.

Our findings suggest that TCF7L2 stabilization of GATA6 after injury is accounted for by reducing PDGFR β protein and diminishing JNK activation. Mechanistically, Wnt activation inhibits PDGF signaling by promoting PDGFR β ubiquitination.³⁶ We also show that TCF7L2 binds a promoter region of GATA6 and activates its transcription. These effects are particularly evident when TCF7L2 is abundant and overcomes the effect of injury, which potently represses expression of GATA6.⁴² Our findings elucidate a previously unrecognized molecular interaction between these transcription factors and identify TCF7L2 as a novel regulator of GATA6-dependent VSMC phenotypic switching.

VSMC have high degree plasticity,⁴⁻⁶ which under pathological conditions allows them to migrate into the intima where they continue proliferating and depositing extracellular matrix⁷ or transdifferentiate into other cell types such as CD68 positive and foam cells.⁸ Although it has been suggested that VSMC proliferation may be beneficial for plaque stability, our rescue of arterial disease in *LRP6^{R611C}* mutant mice by TCF7L2 overexpression and reduced VSMC proliferation is indicative of a context-dependent role. This is a critical subject, as GWAS have associated genetic variants in genes encoding VSMC-specific protein with CAD risk.⁴³ Because *LRP6^{R611C}* mutant mice are also prone to coronary and aortic intimal hyperplasia characterized by medial and intimal thickening in the absence of significant macrophage accumulation, it would be of interest to determine the role of TCF7L2 in atherogenesis versus fibrous cap formation in this model in future studies.

During early embryogenesis and in adult stem cells, TCF7L2 activates cell cycle and promotes cell proliferation.¹⁶ This has led to the conventional wisdom that TCF7L2 promotes VSMC proliferation. Our investigation showed that TCF7L2 inhibits cell cycle activation in VSMCs by upregulating p-P53 and its downstream effector P16. Strikingly, GATA6 has been also shown to increase the expression of p53 and induce growth inhibition in VSMCs.³²

Our study also raises several important questions that require future investigations. These include how does injury or PDGF-BB downregulate TCF7L2 and whether TCF7L2 effects are cell autonomous or noncell autonomous? Such questions may be better addressed in tissue-specific *TCF7L2* knockout mice. One should bear in mind that tissue-specific models may develop completely different traits than those observed in humans simply because the TCF7L2 GWAS-variants are germline polymorphisms, and the associated traits may result from complex interaction between different organs and tissues that express these genetic variants. In this regard,

the generation of TCF7L2 global haploinsufficient or overexpressing mice was an essential step to account for the potential large-scale effects of TCF7L2 variants.

In summary, our study unravels the role of TCF7L2 in regulation of VSMC plasticity and protection against arterial disease. Our earlier work had uncovered the role of TCF7L2 in regulation of plasma lipids¹⁸ and glucose.¹⁹ Collectively, our findings underscore the important role of TCF7L2 as a link between metabolic traits and arterial disease and identifies it as an important target for development of drugs to combat T2DM, metabolic syndrome and its vascular complications.

Acknowledgements

The Genotype-Tissue Expression (GTEx) Project was supported by the Common Fund of the Office of the Director of the National Institutes of Health, and by NCI (National Cancer Institute), NHGRI (National Human Genome Research Institute), NHLBI (National Heart, Lung, and Blood Institute), NIDA (National Institute on Drug Abuse), NIMH (National Institute of Mental Health), and NINDS (National Institute of Neurological Disorders and Stroke). The data used for the analyses described in this article were obtained from: [http://www.gtexportal.org/home/?geneId=TCF7L2], the GTEx Portal on October 28, 2015. TCF7L2 (transcription factor 7-like 2)-bac transgenic and heterozygote TCF7L2 knockout mice were generous gifts from M. Nobrega from University of Chicago.

Sources of Funding

The study was funded by R35 HL135767 grant from National Institutes of Health to A. Mani.

Disclosures

None.

References

- Martín-Timón I, Sevillano-Collantes C, Segura-Galindo A, Del Cañizo-Gómez FJ. Type 2 diabetes and cardiovascular disease: have all risk factors the same strength? *World J Diabetes*. 2014;5:444–470. doi: 10.4239/wjcd.v5.i4.444
- Motterle A, Pu X, Wood H, Xiao Q, Gor S, Ng FL, Chan K, Cross F, Shohreh B, Poston RN, Tucker AT, Caulfield MJ, Ye S. Functional analyses of coronary artery disease associated variation on chromosome 9p21 in vascular smooth muscle cells. *Hum Mol Genet*. 2012;21:4021–4029. doi: 10.1093/hmg/dds224
- Nurnberg ST, Cheng K, Raiesdana A, et al. Coronary artery disease associated transcription factor TCF21 regulates smooth muscle precursor cells that contribute to the fibrous cap. *Genom Data*. 2015;5:36–37. doi: 10.1016/j.gdata.2015.05.007
- Majesky MW, Dong XR, Hoglund V, Daum G, Mahoney WM Jr. The adventitia: a progenitor cell niche for the vessel wall. *Cells Tissues Organs*. 2012;195:73–81. doi: 10.1159/000331413
- Majesky MW, Dong XR, Regan JN, Hoglund VJ. Vascular smooth muscle progenitor cells: building and repairing blood vessels. *Circ Res*. 2011;108:365–377. doi: 10.1161/CIRCRESAHA.110.223800
- Rensen SS, Doevendans PA, van Eys GJ. Regulation and characteristics of vascular smooth muscle cell phenotypic diversity. *Neth Heart J*. 2007;15:100–108.
- Owens GK, Kumar MS, Wamhoff BR. Molecular regulation of vascular smooth muscle cell differentiation in development and disease. *Physiol Rev*. 2004;84:767–801. doi: 10.1152/physrev.00041.2003
- Shankman LS, Gomez D, Cherepanova OA, Salmon M, Alencar GF, Haskins L, Swiatlowska P, Newman AA, Greene ES, Straub AC, Isakson B, Randolph GJ, Owens GK. KLF4-dependent phenotypic modulation of smooth muscle cells has a key role in atherosclerotic plaque pathogenesis. *Nat Med*. 2015;21:628–637. doi: 10.1038/nm.3866
- Arbustini E, Dal Bello B, Morbini P, Burke AP, Bocciarelli M, Specchia G, Virmani R. Plaque erosion is a major substrate for coronary thrombosis in acute myocardial infarction. *Heart*. 1999;82:269–272.

10. Clevers H, Nusse R. Wnt/ β -catenin signaling and disease. *Cell*. 2012;149:1192–1205. doi: 10.1016/j.cell.2012.05.012
11. Srivastava R, Zhang J, Go GW, Narayanan A, Nottoli TP, Mani A. Impaired LRP6-TCF7L2 activity enhances smooth muscle cell plasticity and causes coronary artery disease. *Cell Rep*. 2015;13:746–759. doi: 10.1016/j.celrep.2015.09.028
12. Muendlein A, Saely CH, Geller-Rhomberg S, Sonderegger G, Rein P, Winder T, Beer S, Vonbank A, Drexel H. Single nucleotide polymorphisms of TCF7L2 are linked to diabetic coronary atherosclerosis. *PLoS One*. 2011;6:e17978. doi: 10.1371/journal.pone.0017978
13. Sousa AG, Marquezine GF, Lemos PA, Martinez E, Lopes N, Hueb WA, Krieger JE, Pereira AC. TCF7L2 polymorphism rs7903146 is associated with coronary artery disease severity and mortality. *PLoS One*. 2009;4:e7697. doi: 10.1371/journal.pone.0007697
14. Grant SF, Thorleifsson G, Reynisdottir I, et al. Variant of transcription factor 7-like 2 (TCF7L2) gene confers risk of type 2 diabetes. *Nat Genet*. 2006;38:320–323. doi: 10.1038/ng1732
15. He L, Kernogitski Y, Kulminkaya I, Loika Y, Arbeev KG, Loiko E, Bagley O, Duan M, Yashkin A, Ukraintseva SV, Kovtun M, Yashin AI, Kulminkaya AM. Pleiotropic meta-analyses of longitudinal studies discover novel genetic variants associated with age-related diseases. *Front Genet*. 2016;7:179. doi: 10.3389/fgene.2016.00179
16. Wang X, Xiao Y, Mou Y, Zhao Y, Blankesteyn WM, Hall JL. A role for the beta-catenin/T-cell factor signaling cascade in vascular remodeling. *Circ Res*. 2002;90:340–347.
17. Savic D, Ye H, Aneas I, Park SY, Bell GI, Nobrega MA. Alterations in TCF7L2 expression define its role as a key regulator of glucose metabolism. *Genome Res*. 2011;21:1417–1425. doi: 10.1101/gr.123745.111
18. Go GW, Srivastava R, Hernandez-Ono A, Gang G, Smith SB, Booth CJ, Ginsberg HN, Mani A. The combined hyperlipidemia caused by impaired Wnt-LRP6 signaling is reversed by Wnt3a rescue. *Cell Metab*. 2014;19:209–220. doi: 10.1016/j.cmet.2013.11.023
19. Singh R, De Aguiar RB, Naik S, Mani S, Ostadsharif K, Wencker D, Sotoudeh M, Malekzadeh R, Sherwin RS, Mani A. LRP6 enhances glucose metabolism by promoting TCF7L2-dependent insulin receptor expression and IGF receptor stabilization in humans. *Cell Metab*. 2013;17:197–209. doi: 10.1016/j.cmet.2013.01.009
20. Ray JL, Leach R, Herbert JM, Benson M. Isolation of vascular smooth muscle cells from a single murine aorta. *Methods Cell Sci*. 2001;23:185–188.
21. Wang H, Zhang W, Tang R, Hebbel RP, Kowalska MA, Zhang C, Marth JD, Fukuda M, Zhu C, Huo Y. Core2 1-6-N-glucosaminyltransferase-I deficiency protects injured arteries from neointima formation in ApoE-deficient mice. *Arterioscler Thromb Vasc Biol*. 2009;29:1053–1059. doi: 10.1161/ATVBAHA.109.187716
22. Bennett MR, Sinha S, Owens GK. Vascular smooth muscle cells in atherosclerosis. *Circ Res*. 2016;118:692–702. doi: 10.1161/CIRCRESAHA.115.306361
23. Korinek V, Barker N, Moerer P, van Donselaar E, Huls G, Peters PJ, Clevers H. Depletion of epithelial stem-cell compartments in the small intestine of mice lacking Tcf-4. *Nat Genet*. 1998;19:379–383. doi: 10.1038/1270
24. Pei H, Wang Y, Miyoshi T, Zhang Z, Matsumoto AH, Helm GA, Tellides G, Shi W. Direct evidence for a crucial role of the arterial wall in control of atherosclerosis susceptibility. *Circulation*. 2006;114:2382–2389. doi: 10.1161/CIRCULATIONAHA.106.640185
25. Wilson E, Mai Q, Sudhir K, Weiss RH, Ives HE. Mechanical strain induces growth of vascular smooth muscle cells via autocrine action of PDGF. *J Cell Biol*. 1993;123:741–747.
26. Marmur JD, Poon M, Rossikhina M, Taubman MB. Induction of PDGF-responsive genes in vascular smooth muscle. Implications for the early response to vessel injury. *Circulation*. 1992;86(suppl 6):III53–III60.
27. Stark GR, Taylor WR. Analyzing the G2/M checkpoint. *Methods Mol Biol*. 2004;280:51–82. doi: 10.1385/1-59259-788-2:051
28. Stark GR, Taylor WR. Control of the G2/M transition. *Mol Biotechnol*. 2006;32:227–248. doi: 10.1385/MB:32:3:227
29. Gire V, Dulic V. Senescence from G2 arrest, revisited. *Cell Cycle*. 2015;14:297–304. doi: 10.1080/15384101.2014.1000134
30. Zhou Y, Zhang E, Berggreen C, Jing X, Osmark P, Lang S, Cilio CM, Göransson O, Groop L, Renström E, Hansson O. Survival of pancreatic beta cells is partly controlled by a TCF7L2-p53-p53INP1-dependent pathway. *Hum Mol Genet*. 2012;21:196–207. doi: 10.1093/hmg/ddr454
31. Wada H, Hasegawa K, Morimoto T, Kakita T, Yanazume T, Sasayama S. A p300 protein as a coactivator of GATA-6 in the transcription of the smooth muscle-myosin heavy chain gene. *J Biol Chem*. 2000;275:25330–25335. doi: 10.1074/jbc.M000828200
32. Perlman H, Suzuki E, Simonson M, Smith RC, Walsh K. GATA-6 induces p21(Cip1) expression and G1 cell cycle arrest. *J Biol Chem*. 1998;273:13713–13718.
33. Suzuki E, Evans T, Lowry J, Truong L, Bell DW, Testa JR, Walsh K. The human GATA-6 gene: structure, chromosomal location, and regulation of expression by tissue-specific and mitogen-responsive signals. *Genomics*. 1996;38:283–290. doi: 10.1006/geno.1996.0630
34. Reusch P, Wagdy H, Reusch R, Wilson E, Ives HE. Mechanical strain increases smooth muscle and decreases nonmuscle myosin expression in rat vascular smooth muscle cells. *Circ Res*. 1996;79:1046–1053.
35. Holycross BJ, Blank RS, Thompson MM, Peach MJ, Owens GK. Platelet-derived growth factor-BB-induced suppression of smooth muscle cell differentiation. *Circ Res*. 1992;71:1525–1532.
36. Keramati AR, Singh R, Lin A, Faramarzi S, Ye ZJ, Mane S, Tellides G, Lifton RP, Mani A. Wild-type LRP6 inhibits, whereas atherosclerosis-linked LRP6R61C increases PDGF-dependent vascular smooth muscle cell proliferation. *Proc Natl Acad Sci USA*. 2011;108:1914–1918. doi: 10.1073/pnas.1019443108
37. Hatzis P, van der Flier LG, van Driel MA, Guryev V, Nielsen F, Denissov S, Nijman JJ, Koster J, Santo EE, Welboren W, Versteeg R, Cuppen E, van de Wetering M, Clevers H, Stunnenberg HG. Genome-wide pattern of TCF7L2/TCF4 chromatin occupancy in colorectal cancer cells. *Mol Cell Biol*. 2008;28:2732–2744. doi: 10.1128/MCB.02175-07
38. Ushijima H, Maeda M. cAMP-dependent proteolysis of GATA-6 is linked to JNK-signaling pathway. *Biochem Biophys Res Commun*. 2012;423:679–683. doi: 10.1016/j.bbrc.2012.06.013
39. Davidson G, Shen J, Huang YL, Su Y, Karaulanov E, Bartscherer K, Hassler C, Stannek P, Boutros M, Niehrs C. Cell cycle control of wnt receptor activation. *Dev Cell*. 2009;17:788–799. doi: 10.1016/j.devcel.2009.11.006
40. Mani A, Radhakrishnan J, Wang H, Mani A, Mani MA, Nelson-Williams C, Carew KS, Mane S, Najmabadi H, Wu D, Lifton RP. LRP6 mutation in a family with early coronary disease and metabolic risk factors. *Science*. 2007;315:1278–1282. doi: 10.1126/science.1136370
41. Bienz M. TCF: transcriptional activator or repressor? *Curr Opin Cell Biol*. 1998;10:366–372.
42. Mano T, Luo Z, Malendowicz SL, Evans T, Walsh K. Reversal of GATA-6 downregulation promotes smooth muscle differentiation and inhibits intimal hyperplasia in balloon-injured rat carotid artery. *Circ Res*. 1999;84:647–654.
43. Liu B, Pjanic M, Wang T, Nguyen T, Gloudemans M, Rao A, Castano VG, Nurnberg S, Rader DJ, Elwyn S, Ingelsson E, Montgomery SB, Miller CL, Quertermous T. Genetic regulatory mechanisms of smooth muscle cells map to coronary artery disease risk loci. *Am J Hum Genet*. 2018;103:377–388. doi: 10.1016/j.ajhg.2018.08.001

Highlights

- Vascular Smooth muscle cell plasticity renders them with a unique capability to dedifferentiate and proliferate under pathological conditions, resulting in formation of intimal hyperplasia.
- Altered function of Wnt coreceptor LRP6 has been implicated in intimal hyperplasia.
- The genetic variants of Wnt-regulated transcription factor TCF7L2 (transcription factor 7-like 2) have been associated with susceptibility to type 2 diabetes mellitus and coronary artery disease, but their mechanisms of action are not known
- In vivo studies indicate that TCF7L2 upregulates GATA6 (GATA-binding protein 6), jointly promotes vascular Smooth muscle cell differentiation and reduces vascular Smooth muscle cell proliferation.
- The overexpression of TCF7L2 is protective while its reduced expression promotes intimal hyperplasia.